https://doi.org/10.5194/egusphere-2026-2097
Preprint. Discussion started: 21 May 2026
© Author(s) 2026. CC BY 4.0 License.

On the calibration and monitoring of dual-polarization radar receivers operating at C-band using solar flux reference at S-band

Andrea Francesco Battaglia[1] and Marco Gabella[2]

[1]Istituto ricerche solari Aldo e Cele Daccò (IRSOL), via Patocchi 57, 6605 Locarno-Monti, Switzerland
[2]MeteoSwiss, via ai Monti 146, 6605 Locarno-Monti, Switzerland

Correspondence: Andrea Francesco Battaglia (andrea.francesco.battaglia@irsol.usi.ch)

Abstract. The solar radio noise accurately measured by terrestrial solar observatories has been proved to be an effective reference for checking the quality of dual-polarization weather radar receivers. The longest, most complete and accurate record of solar spectral irradiance ("flux", for the sake of brevity) values exists thanks to the Dominion Radio Astrophysical Observatory (DRAO) of the National Research Council (NRC) of Canada, located in British Columbia. Solar flux measurements acquired by DRAO at 2.8 GHz represent a valuable and useful basis for the calibration of radar receivers. In Europe the large majority of weather radars operates between 5.4 and 5.6 GHz. To be rigorous, one needs measurements of solar radio noise at the same frequency of the weather radar. If one is prepared to accept some uncertainty, it is possible to extrapolate solar flux values from S- to C-band. The formula proposed by Tapping (2001) is widely used in Europe: it is based on a constant scaling factor to predict the flux at the higher frequency from the measured flux at 2.8 GHz, after having subtracted the quiet component at both frequencies. We have analyzed 240 quality-checked, 1-hour lasting solar flux measurements, simultaneously acquired at S- and C-band by the Expanded Owens Valley Solar Array (EOVSA) observatory during the current XXV solar cycle and empirically derived the optimal value of the scaling factor for the conversion from S- to C-band. We found that there is a clear non-linear dependence between this variable scaling factor and the slowly varying solar component. Thanks to the new conversion formula, which is based on the variable scaling factor, the agreement between C-band radar observations in Europe and DRAO-converted reference values improved both in relative and in absolute terms. Not much can be done to compensate the shift in time between measurements in Europe vs DRAO (noon at 20 UTC). Our recommendation is that of developing and installing an optimized C-band radio telescope in Europe tailored to radar calibration purposes.

1 Introduction

Proper adjustment of the antenna pointing and receiver chain calibration is of crucial importance for weather radar performance. For such purposes, one of the best reference tool is certainly the Sun. This bright source of radio noise is definitely in the far field of the antenna; the corresponding measurements can be consistent and accurate. In addition, the same bright source can be detected simultaneously over a huge geographic area, making it possible to tie together the calibration of many systems at the same, ideal, noon time. The most important prerequisite for antenna and radar receiver calibration is that accurate reference measurements are acquired by a radio telescope at the operating frequency of the radar, especially if the Sun is not quiet, which

https://doi.org/10.5194/egusphere-2026-2097
Preprint. Discussion started: 21 May 2026
© Author(s) 2026. CC BY 4.0 License.

is during most of its 11-year fluctuations period. The availability of a synchronous reference measurement of solar spectral irradiance is the second most important prerequisite.

A very long record of accurate measurements of solar spectral irradiance exists thanks to the Dominion Radio Astrophysical Observatory (DRAO) of the National Research Council of Canada, which is located in British Columbia (BC) at $\sim 50^{\circ}$ latitude (noon around 20 UTC). Since it goes back to 1947, such data set is highly precious, with a unique climatological and historical value. Since 1996, three 1-hour lasting, accurate determinations of the solar "flux" measurements are performed every day by DRAO, namely at 17, 20 and 23 UTC (Tapping, 2013). The operating frequency is 2.8 GHz (10.7 cm wavelength), namely within the S-band. This frequency is particularly useful for weather radars in North America, where most systems operate at S-band, but not for weather radars in Europe, China and Oceania (mainly C-band) or Japan and India (mainly X-band). It has become clear that S-band frequencies are optimal for monitoring the activity of the Sun because emissions in this band are sensitive to conditions in the upper solar chromosphere and at the base of the corona (e.g., Benz, 2009). However, the choice of a wavelength of 10.7 cm, which lies in the history of radar development during the Second World War, was purely serendipitous. Consequently, in addition to be a freely available and widely used reference datum for radar receiver calibration, the solar radio flux has become also one of the most widely used index of solar activity. Its applications include the usage as a simple and straightforward solar activity level indicator, as well as a proxy for other solar characteristics (e.g., sunspot number) or quantities that are more difficult to obtain.

The first attempts to calibrate the antenna of weather radars using the Sun date back to the late 1970s with the efforts by Frush and Lewis at the National Center for Atmospheric Research (S-band radar); preliminary results were presented in 1984 using values of DRAO and of the US Air Force Radio Solar Telescope Network (RSTN) for a qualitative comparison (Frush, 1984). The results of a successful quantitative comparison have been presented five years later by Pratte and Ferraro (1989): their analysis was based on 14 accurate "Sun-Track" (see Sect. 2.2) measurements acquired during the active solar period between November 1987 and August 1988; the reference solar flux values were those acquired in Ottawa (at that time) by DRAO, ranging from 19.8 to 22.6 dBsfu, with a standard deviation of 0.78 dB. DRAO solar flux measurements at S-band have been used as reference also by several Radio Astrophysical Observatories worldwide for their radio telescopes operating at 2.8 GHz, e.g. the 4 sites of the Radio Solar Telescope Network (RSTN; Guidice et al., 1981; Giersch and Kennewell, 2022), the Korean site in Icheon (Yun et al., 2014), and the Expanded Owens Valley Solar Array (EOVSA; Gary et al., 2018; Shaik and Gary, 2021) located in California.

What about weather radars working at other frequencies than S-band? In order to estimate the flux at nearby bands (for instance, C-band), Tapping has proposed already in 2001 an effective and simple formula (Tapping, 2001) at the AMS calibration workshop held in Albuquerque. Such formula, which requires a priori knowledge of the quiet solar component at S-band and C-band, is based on a fixed scaling factor for the prediction of the value at C-band (see also Sect. 3.1) from the accurate measured value at S-band. In Europe, such a formula was introduced in 2004 at KNMI (Holleman and Beekhuis, 2004). Then, it has become popular and widely used, thanks to the idea of using the solar signal detected by ground-based radars during the operational weather scan program ("Sun-check", see Sect. 2.2), which has been presented in a series of papers: Huuskonen and Holleman (2007) have proposed the use of solar signals to determine antenna pointing. Holleman et al. (2010b) have extended

https://doi.org/10.5194/egusphere-2026-2097
Preprint. Discussion started: 21 May 2026
© Author(s) 2026. CC BY 4.0 License.

the method towards quantitative electromagnetic power measurements, aiming at monitoring radar receiving chain stability: the analysis was based on data from two single polarization radars in the Netherlands during an active (year 2005) and quiet (year 2008) period. In the case of dual-polarization radars, which are able to measure both horizontal (H) and vertical (V) polarization, the same technique can be used to monitor the absence (or presence) of a residual differential reflectivity offset: the stability of differential radar reflectivity was investigated by Holleman et al. (2010a) during a period of quiet Sun emissions (three months in 2008 using a dual-polarization radar in France) and by Gabella (2015) during high solar activity (the first 224 days, approximately 8 solar rotations, in 2014, using the three Swiss radars available at that time). In 2017, Gabella et al. (2017) have presented an analysis based on 6 radars and 100 relatively active days: the variability of all the 6 radars was larger than the one predicted by the formula. Consequently, it was possible to improve the agreement between each radar and the prediction simply by increasing the value of the scaling factor; the effect of such an adjustment was that of increasing the variability of the DRAO reference at C-band to bring it closer to the one measured by the six radars. The authors pointed out two limitations: the augmented value of the scaling factor during that specific active period was empirically derived a posteriori without any link to a physical model; the new scaling factor affected not only the variability of the reference (dispersion of the solar signal around the mean value) but also the mean value itself. This fact sounded particularly unsatisfactory to the authors: a modification conceived to improve only the relative calibration was also affecting the absolute calibration.

In the present manuscript, on the contrary, we present a physical model where the scaling factor depends on the solar activity measured at the reference frequency, which is at 2.8 GHz (S-band). This assumption is then verified thanks to simultaneous S- and C-band measurements by EOVSA, which are acquired at the same time of DRAO, corresponding to local noon. The article is organized as follows. in Sect. 2 we present the data and instruments used in this study. In Sect. 3 we review the model of Tapping (2001) and propose our new models. The application of these models to operational weather radars in terms of both relative and absolute calibration is presented in the results section (Sect. 4). Discussions and conclusions are presented in Sect. 5 and in Sect. 6, respectively.

2 Data and instrumentation

For the microwave solar flux analysis presented in this paper, we have considered solar flux measurements from DRAO and EOVSA spanning 240 days within solar cycle XXV, from early 2020 to early 2025. Thanks to the spectral information provided by EOVSA, we were able to test the model of Tapping (2001) for estimating the solar flux at C-band (5.5 cm, 5.45 GHz) from observations at S-band (10.7 cm, 2.8 GHz) and to develop improved models (see more details in Sect. 3.2). These new models were then tested using meteorological weather radar data. The following two sub-sections describe the reference data (DRAO and EOVSA) and those of the devices under test.

https://doi.org/10.5194/egusphere-2026-2097
Preprint. Discussion started: 21 May 2026
© Author(s) 2026. CC BY 4.0 License.

2.1 DRAO and EOVSA data

The daily DRAO solar flux data at 2.8 GHz are available through the Space Weather Canada portal[1]. For our analysis, we considered only observations around local noon (20:00 UTC) and used the measured flux values. A detailed description of the DRAO solar flux monitors is provided by Tapping (2013).

EOVSA is an interferometric array of 13 antennas, each 2.1 m in diameter, providing measurements of the solar microwave spectrum between 2.5 GHz (12 cm) and 18 GHz (1.7 cm), with approximately 40 MHz frequency resolution, and a cadence of one second. The data we used for the analysis corresponds to the publicly accessible daily synoptic solar observations[2]. The flux calibration of EOVSA (Shaik and Gary, 2021) relies on solar flux measurements from RSTN and DRAO, as reported by the NOAA. Because EOVSA provides continuous spectral information between the DRAO reference frequency of 2.8 GHz and the frequency of 5.45 GHz used by the Swiss meteorological weather radars, we consider EOVSA to be a suitable instrument for testing the model of Tapping (2001).

The selected days for the analysis span the entire current solar cycle, except for the period from early to mid 2023, during which no data could be collected due to a major technical problem at EOVSA. To derive the EOVSA spectrum for a selected day, we consider hourly average values around local noon, corresponding to 19:00 - 20:00 UTC. The integration time of EOVSA is occasionally adjusted within a ± 30 min window to avoid data gaps caused by calibration measurements. For the selection of the days to include in our analysis, we also verified the absence of moderate to major flares within the considered time interval, then that our frequencies of interest did not exhibit any instrumental artifacts. In total, we have collected 240 daily sampling values in a 6-year period (2020-2025) of the current cycle, to capture the evolution of solar activity, from quiet periods (2020) to the current decreasing period (through the "strongest peak period" in 2024), driven by the enhanced and varying microwave emission from sunspots (see Fig. 1).

2.2 Swiss operational radar data

As stated in the introduction, the Solar radio noise accurately measured by terrestrial solar observatories has been proved to be an effective reference for checking the quality of dual-polarization, ground-based, weather radar receivers. Measurements of the solar radio noise are useful not only for monitoring and for relative calibration, but also for absolute calibration. Two complementary methodologies are currently used in Switzerland to retrieve quantitative estimate of the solar spectral irradiance (solar flux values) from observations by the dual-polarization, operational C-band weather radars:

A) Fully automatic monitoring based on the analysis of a large number of “noisy” solar signals (“hits”) in the polar volume reflectivity data produced during the operational weather scan program (Holleman et al., 2010a, b; Gabella, 2015; Huuskonen et al., 2016). At MeteoSwiss, we use the term “Sun-Check” to refer to this method. The Sun-check has become now a crucial routine for the daily monitoring of dual-polarization receivers as well as for the quantitative assessment of the relative calibration (see Sect. 4.2).

[1] https://www.spaceweather.gc.ca/forecast-prevision/solar-solaire/solarflux/sx-5-en.php (accessed 2025-12-09).
[2] https://www.ovsa.njit.edu/wiki/index.php/EOVSA_Data_Products (accessed 2025-12-09).

https://doi.org/10.5194/egusphere-2026-2097
Preprint. Discussion started: 21 May 2026
© Author(s) 2026. CC BY 4.0 License.

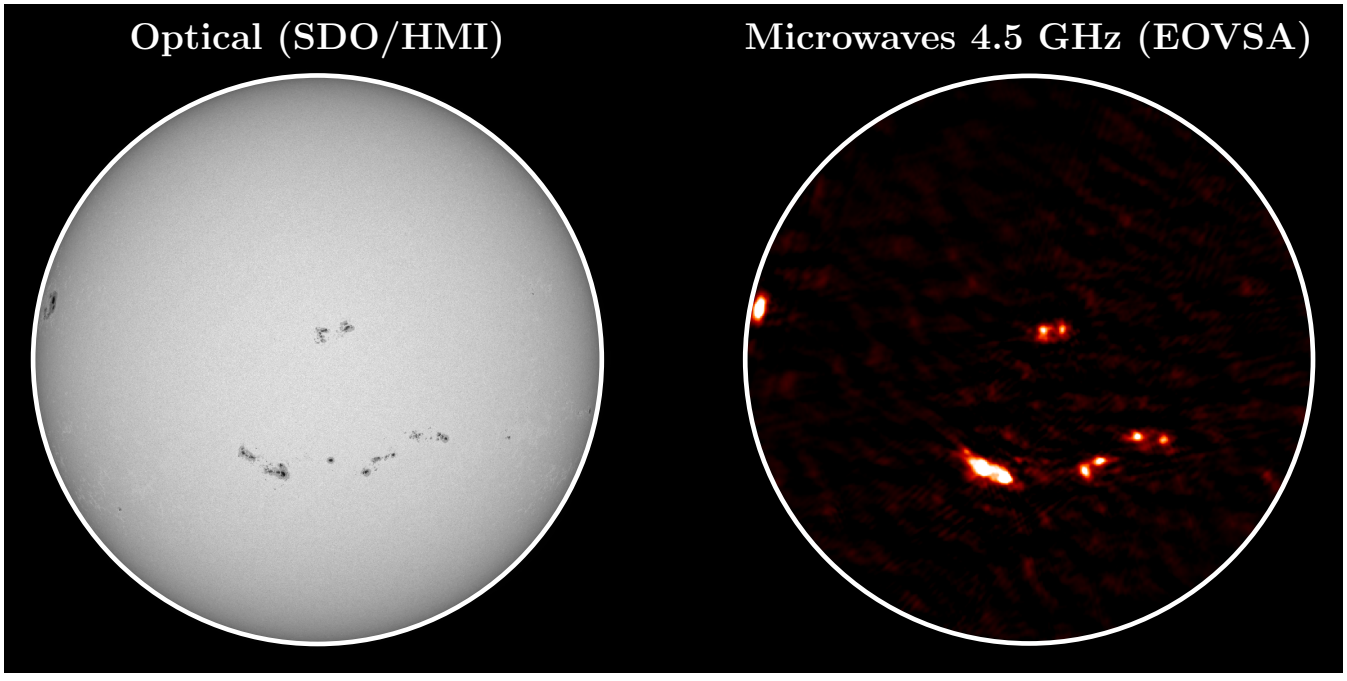

Figure 1. Optical (left) and microwave (at 4.5 GHz, right) images of the Sun on 2024-10-02. This figure illustrates the strong correspondence between sunspots, which are regions of intense magnetic fields, and the bright regions observed in microwaves. Through the differential rotation of the Sun, these regions define the slowly-varying component measured in microwave observations. A movie showing the temporal evolution of these images and illustrating the slowly-varying component is available online.

B) Special-purpose, manual, "long-lasting" (some tens of seconds) observations with maximized Sun-to-Noise ratio, where the dedicated observations are obtained by pointing (and tracking) the antenna beam axis at the center of the solar disk. At MeteoSwiss, we use the term "Sun-Track" to refer to this more accurate, on-demand method, developed for absolute calibration purposes (Gabella, 2015). These measurements are obviously performed during clear sky conditions and close to the local noon.

The main disadvantage of the Sun-Track method (B) is that the radar has to be off-line during the dedicated solar observation. Typically five close-in-time, consecutive observations are used to derive a reference value; hence, the radar is out of the composite for 5-7 minutes, all included. Nevertheless, the time devoted to point the antenna beam axis at the center of the solar disk, hence maximizing the Sun-to-Noise ratio is crucial. This ratio, in fact, is as small as 7 dB for our operational weather radar operating at C-band when the Sun is quiet. For the MeteoSwiss radars, Sun-Track is run manually a couple of times per year during clear sky conditions and a relative minimum of the slowly varying component. However, for a non-operational X-band radar on wheel, Gabella and Leuenberger (2017) have implemented a weather scan program that includes fully automatic, 30-min, Sun-track observations.

https://doi.org/10.5194/egusphere-2026-2097
Preprint. Discussion started: 21 May 2026
© Author(s) 2026. CC BY 4.0 License.

On the contrary, with the Sun-Check method (A), a large number of "noisy" solar signals ("hits") in the polar volume reflectivity data produced during the operational weather scan program are collected. These signals are "noisy" in the sense that the Sun-to-Noise ratio can be as small as a few dB in cases where the beam axis is at the edge of the solar disk; for many Sun "hits", in fact, the angular distance between the antenna beam axis and the center of the solar disk is of the order of 0.4-0.7 degrees. This explains why the Sun-to-Noise ratio is significantly worse than with Sun-Track. Consequently, for retrieving a daily value of solar spectral irradiance, several tens of hits are used: at first, an estimated level of Noise is subtracted from the received Sun-plus-Noise signal; then, noise-subtracted values are fitted using the Gaussian antenna deconvolution method described in Holleman and Beekhuis (2004). Once the 5 parameters of the paraboloid are derived (for instance, by means of the least squares method), the "maximized" solar power that the radar would have received, if the beam had hit the center of the Sun, is retrieved. Given this level of complexity, at MeteoSwiss we do not attempt any absolute calibration (see Sect. 4.3) based on Sun-Check values; however, they are necessary and fundamental for the daily monitoring of dual-polarization receivers as well as for the quantitative assessment of relative calibration (see Sect. 4.2).

In both cases, Sun-Track and Sun-Check techniques, the solar flux values here reported in sfu are double the actual measured values, because the radar measurements are acquired through separate, orthogonal linear polarizations. The solar radio flux, in fact, just like the predominant emission in the visible part of the electromagnetic spectrum, is in most cases randomly polarized. Exceptions are solar storms, since the emission of some localized active regions shows circular polarization. However, even in such cases, the two orthogonal, linearly polarized receiver waveguides will again intercept one half of the radiated power.

3 Models

3.1 The model of Tapping (2001) for solar flux estimation

Several attempts have been made in the past to model the slowly-varying component (see Fig. 1) of solar radio flux (e.g., Kennewell, 1989), enabling the estimation of flux density at desired frequencies from 1 to 20 GHz based on the DRAO flux measurements. However, a recent analysis (Giersch and Kennewell, 2022) reported that some models exhibit significant deviations from observed data, limiting their practical applicability. Another approach has been proposed by Tapping (2001), which has shown improved agreement with observations. This model is being adopted operationally for weather radar systems in Europe in order to provide the reference solar flux density at C-band from DRAO S-band measurements. In the following, we summarize the main principles and key aspects of such model.

The model proposed by Tapping (2001) estimates solar flux at wavelengths different from the flux at 10.7 cm (2.8 GHz frequency) measured at DRAO, leveraging the stability of the spectrum of the slowly-varying component in solar activity. This method achieves an accuracy within approximately 1 dB (Tapping, 2001). The approach is built upon the following assumptions:

- In the absence of flares, solar emission at centimeter wavelengths consists of two distinct components: a steady baseline level (the quiet Sun) and a slowly-varying component (associated with active regions, see Fig. 1);

https://doi.org/10.5194/egusphere-2026-2097
Preprint. Discussion started: 21 May 2026
© Author(s) 2026. CC BY 4.0 License.

– As solar activity rises and falls, the amplitude of the spectrum changes while its shape remains nearly unchanged.

The method for estimating the flux density at a wavelength different from 10.7 cm is rather straightforward. First, subtract the quiet Sun flux density at 10.7 cm from the observed DRAO flux to obtain the flux associated with the slowly-varying component. Next, convert this value to the desired wavelength (in our case, 5.5 cm) by multiplying it by the appropriate scaling factor p_λ, whose value depends on the target wavelength. A table summarizing these scaling factors is provided in Tapping (2001). For estimating the flux density at 5.5 cm, $p_\lambda = 0.715$ is used (see Eq. (1) in Gabella, 2015). Finally, obtain the solar flux density at the desired wavelength by adding the quiet Sun value at that wavelength. This process is summarized in the following equation

$$F_\lambda = p_\lambda \left(F_S^{\mathrm{DRAO}} - Q_S\right) + Q_\lambda, \tag{1}$$

where F_S^{DRAO} is the observed flux density by DRAO in the S-band (at 10.7 cm), Q_S is the quiet Sun flux in the S-band (at 10.7 cm, typically assumed to be 64 sfu), Q_λ is the quiet Sun flux at the desired wavelength (at 5.5 cm, typically assumed to be 113 sfu), and F_λ is the estimated flux at the desired wavelength. In this model, p_λ ranges from 0.65 to 1.00, where 1.00 corresponds to the p_λ value at approximately 10.7 cm. This indicates that the model assumes that the spectral peak of the slowly-varying component occurs at around 10.7 cm, exactly where DRAO performs its measurements.

We note that in this model, the scaling factors p_λ are independent of the activity level, meaning that the scaling factor remains constant regardless of whether the measurement is done at solar minimum or maximum. This is because the model assumes that the spectrum of the slowly-varying component scales linearly with activity. In this article, we test this assumption through EOVSA observations and evaluate the influence of a changing spectrum on the estimated flux at a different frequency.

3.2 Derivation of the "variable p_λ" models through the varying microwave spectrum

In Fig. 2 we show the spectra of the slowly-varying component observed by EOVSA for eight example spectra. This figure illustrates that not only the amplitude changes with solar activity, but also the spectral shape shows clear variations, which depend on intrinsic characteristics of the active regions present on the solar disk (e.g., magnetic field strength distributions, see Sect. 5 for more details). These spectral-shape differences can vary on a day-to-day basis, since an active region could evolve significantly within a single day through processes such as new magnetic flux emergence, decay, or partial magnetic restructuring associated with strong activity (i.e., large flares and coronal mass ejections). As a result, the frequency at which the spectral peak of the slowly-varying component occurs, can shift. An example is shown by the orange spectrum in Fig. 2, referring to a date late in 2024 near solar maximum, where the peak does not occur at 2.8 GHz but rather around 3.5–4 GHz. This has some influence on the p_λ parameter. Therefore, this figure shows that the spectrum of the slowly-varying component changes not only in amplitude with activity level but also in shape.

Using the spectra obtained from EOVSA over the selected 240 days, we were able to determine the flux density values at both frequencies of interest (2.8 GHz and 5.45 GHz, at S- and C-band, respectively). With these measurements, we can derive the scaling factor, p_λ, needed to estimate the C-band flux density from the flux density measured at S-band. This is simply

https://doi.org/10.5194/egusphere-2026-2097
Preprint. Discussion started: 21 May 2026
© Author(s) 2026. CC BY 4.0 License.

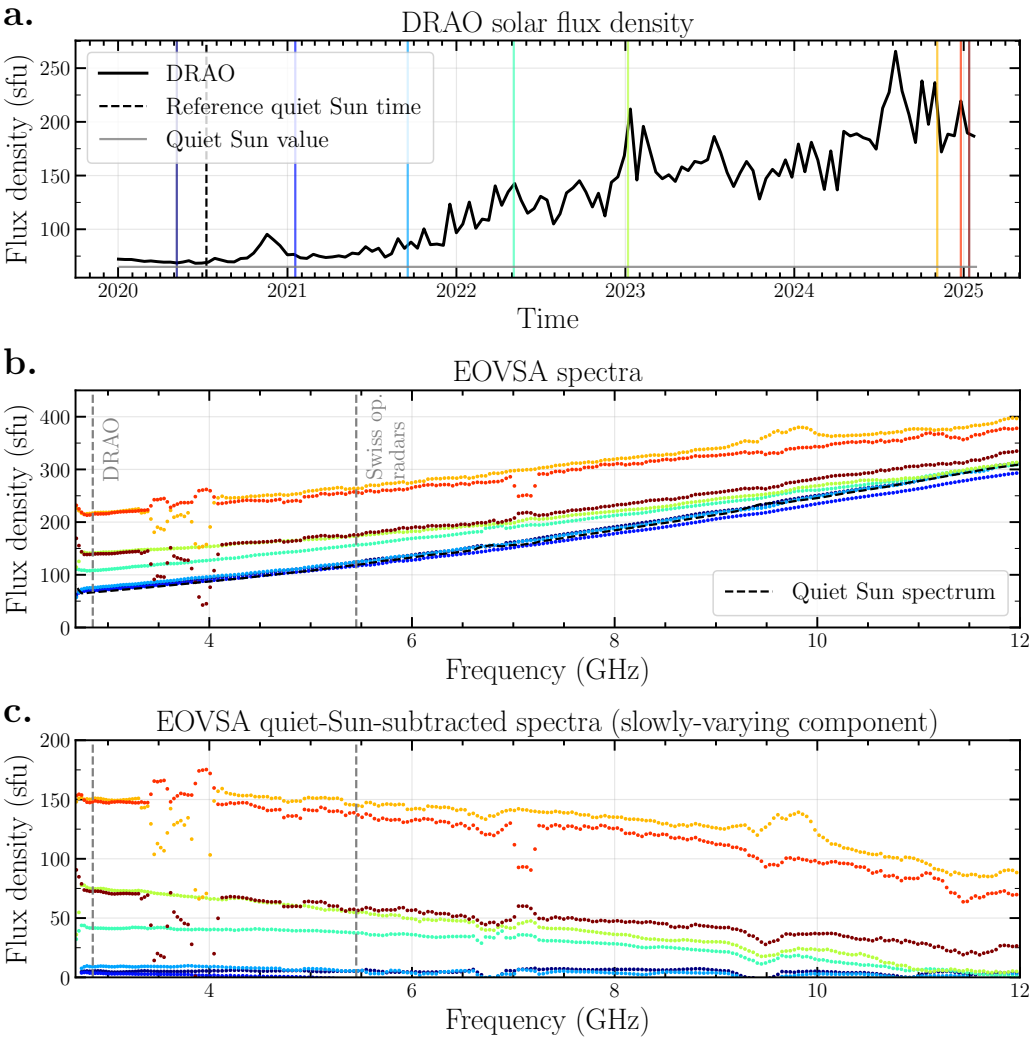

Figure 2. Daily solar flux measurements and eight example microwave spectra. (*a*) Solar flux density at 10.7 cm wavelength (2.8 GHz) measured by DRAO (noon flux only) from early 2020 to early 2025, with a 2-week average. Colored vertical bars indicate time periods corresponding to the spectra shown in the panels below. The vertical dashed black line marks the date of the measurement used as the quiet Sun reference. (*b*) Solar microwave spectra observed with EOVSA, with colors corresponding to the dates in panel (*a*). For reference, the frequencies of DRAO and Swiss operational radars are shown as vertical gray dashed lines. (*c*) Quiet-Sun-subtracted EOVSA spectra highlighting the slowly-varying component. The amplitude of this component varies significantly with solar activity, and the spectral shape also changes, directly affecting the value of p_λ.

https://doi.org/10.5194/egusphere-2026-2097
Preprint. Discussion started: 21 May 2026
© Author(s) 2026. CC BY 4.0 License.

done by reversing Eq. (1), such that

$$p_\lambda = \frac{F_C^{\mathrm{EOVSA}} - Q_C}{F_S^{\mathrm{EOVSA}} - Q_S} \tag{2}$$

with F_S^{EOVSA} and F_C^{EOVSA} the flux density values observed by EOVSA in the S- and C-band, respectively, and Q_S and Q_C the quiet-Sun values in the S- and C-band, respectively (assumed to be 64 sfu and 113 sfu, respectively). The underlying assumption associated with these two fixed quiet-Sun values is that the Sun returns to the same quiet values at the end of each cycle. This assumption is the first factor of uncertainty. To derive p_λ from the same spectrum while avoiding cross-calibration differences between EOVSA and DRAO, we used the flux at S-band, F_S^{EOVSA}, from EOVSA observations.

In Fig. 3 we show how p_λ varies with the solar activity level, where the activity is represented using the solar flux value measured by EOVSA in the S-band (at 2.8 GHz). Indeed, p_λ decreases toward lower values as the solar flux decreases, while p_λ approaches one when solar activity is higher. This fact occurs because the spectral peak of the slowly-varying component lies between the S-band and C-band, as illustrated, for example, by the orange spectrum in Fig. 2.

The trend of p_λ versus the solar activity shown in Fig. 3 is fitted with two models. The first model is a (log-transformed) linear regression, yielding the following coefficients in the equation of the ordinary least-square regression:

$$p_\lambda(F) = 0.714 + 0.929 \cdot X(F), \quad \text{where} \quad X(F) = \log\left(\frac{F_S^{\mathrm{EOVSA}}}{141.2}\right) \tag{3}$$

with F_S^{EOVSA} being the measured flux of EOVSA in the S-band. The choice of a logarithmic scale for the explanatory variable on the abscissa is a consequence of an emerging quasi-exponential trend between p_λ and F_S^{EOVSA}. Consequently, the pattern of the gray dots shows a quasi-linear trend as a function of the normalized, explanatory variable $X(F)$. The explained variance in percentage, defined as 100 times the coefficient of determination, results to be 84.9%. To reduce the uncertainty of the constant term of the linear regression, we have normalized F_S^{EOVSA} around a central value (Wilks, 2011). For logarithmically transformed variables, the geometric mean of the range has provided the normalization factor that minimizes the uncertainty of the central values, which consequently resulted to be 0.714 ± 0.0042. In formulas:

$$F_0 = \sqrt{F_{\min} \cdot F_{\max}} \simeq 141.2\,\mathrm{sfu}. \tag{4}$$

By normalizing F_S^{EOVSA} by such value (141.2 sfu), we also ensure that the intercept has a direct physical interpretation, as it is the expected p_λ at the central value of the flux density range. Interestingly, this normalization yields an intercept of 0.714, remarkably close to the fixed value $p_\lambda = 0.715$ used in the model of Tapping (2001) to estimate C-band flux from S-band flux density measurements. The regression slope uncertainty, which tends to 0 when the correlation coefficient tends to 1, results to be in this case ± 0.025. The residual plot in Fig. 3 (panel *b.*) shows the difference between the optimal value of p_λ and the one derived using the two fit models as a function of the fitted values. The log-transformed model reveals slight systematic patterns in the residuals. At low and high fitted values, the residuals tend to overestimate the flux, while at mid-level values, they slightly underestimate the measured flux.

https://doi.org/10.5194/egusphere-2026-2097
Preprint. Discussion started: 21 May 2026
© Author(s) 2026. CC BY 4.0 License.

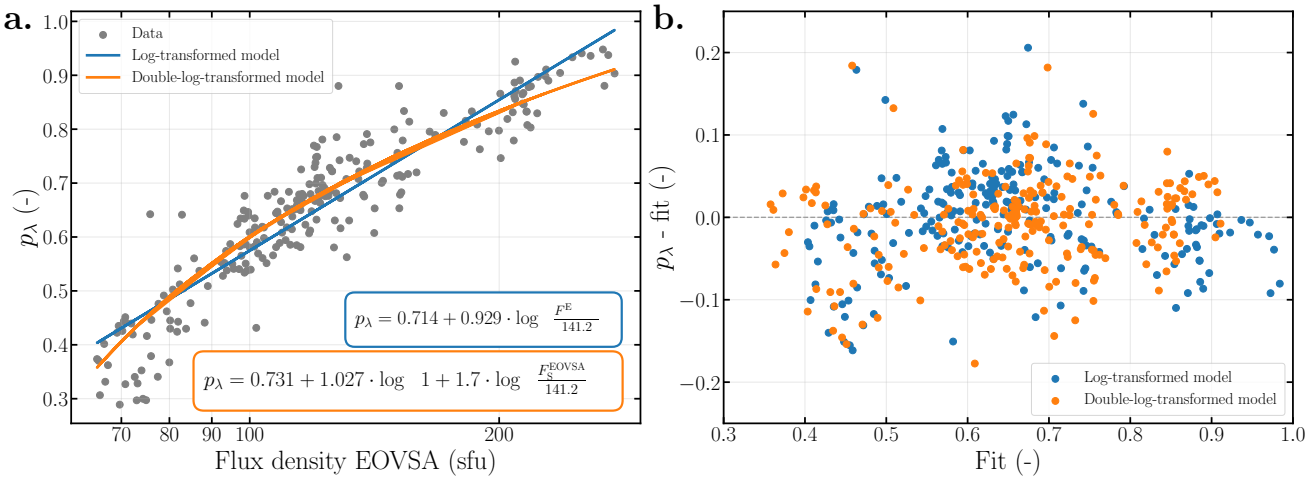

Figure 3. Variation of the p_λ parameter as a function of the solar activity. (*a*) p_λ as a function of the EOVSA flux density at 2.8 GHz (10.7 cm). The blue and orange curves represent two different fits to the data, a log-transformed linear regression and an exponential regression, respectively. The corresponding equations are displayed in the legend. (*b*) Residual plot showing the residuals as a function of the fitted values.

To reduce these slight systematic patterns, we introduce an additional model. This second model assumes a double exponential dependence between the scaling factor and the solar activity at S-band. We call it double-log-transformed model, since it can be expressed through the following linear equation (after a double-log transformation):

$$p_\lambda(F) = 0.731 + 1.027 \cdot W(F), \quad \text{where} \quad W(F) = \log\left(1 + 1.7 \cdot X(F)\right) = \log\left(1 + 1.7 \cdot \log\left(\frac{F_S^{\mathrm{EOVSA}}}{141.2}\right)\right) \tag{5}$$

The explained variance in this case results to be slightly larger, namely 87.9%. In order to derive the model equation, we adopted the same approach as done in Eq. (3), specifically that in order to reduce the uncertainty in the intercept term, we normalized F_S^{EOVSA} around the central value of 141.2 sfu. For this model, the normalization yields a central and most frequent value of 0.731, again close to the value of $p_\lambda = 0.715$ used in the model of Tapping (2001). The residual plot of the double-log-transformed model shows reduced systematic discrepancy at high and low values between the model and the data, with a larger value of the explained variance, which is 87.9% (a bit better than the value of 84.9% obtained using the log-transformed model, 52 degrees of freedom in both cases). In the following, we therefore use both models for application and comparison with operational weather radar measurements.

https://doi.org/10.5194/egusphere-2026-2097
Preprint. Discussion started: 21 May 2026
© Author(s) 2026. CC BY 4.0 License.

4 Results

4.1 Scores for the assessment of the agreement

The models for extrapolating at C-band DRAO accurate solar flux measurements at S-band are quantitatively evaluated in this section in terms of mean “residual error” (actually, radar-model disagreement) and dispersion of such “error” around the mean. As most of radar receiver errors are multiplicative in nature, it is sensible to define the “residual error” as the log-transformed ratio (expressed in dB) between the value measured by the radar and that of the reference model, which converts solar flux values from S-band to C-band. An obvious example of a multiplicative type of error is signal attenuation along the propagation path or by the wet radome, the protection sphere around the radar antenna (Schmid et al., 2025).

The average of the residual error (Bias) in dB is the most important score ("primary") when the focus is on the absolute calibration level, provided that the ("secondary") independent score, which is the standard deviation of the error (also in dB), is reasonably smaller. Indeed, the standard deviation of the error is independent of any systematic bias that could affect the measurements by the radar or by the radio astrophysical reference and it could be taken as an estimate of the uncertainty when the focus is on absolute calibration. It is interesting to give some order of magnitude to set such error in the context of operational radar meteorology: when evaluating the absolute calibration of the radar receiver chain at MeteoSwiss, we consider acceptable a mean error of the order of 1 dB, provided that the uncertainty is within ± 0.4 dB. A detailed example of absolute calibration will be given in Sect. 4.3, using the 20 accurate observations acquired with the Sun-Tracking methodology (see Sect. 2.2) applied to the Albis radar Calibration Unit in the 13-years period 2013-2025.

When the scope of the analysis is on the monitoring of the dual-polarization radar receiver, then the dispersion of the error becomes the crucial score, being in this case the focus on the relative agreement. In this case, the most intuitive score is probably the standard deviation of the error, which, in our daily monitoring case, is defined as the standard deviation of the log-transformed radar-to-model daily ratios. However, being highly sensitive to any single large error due to mismatch in time (think, for instance, of a flare between 23 and 24 UTC, which would be detected by DRAO but certainly could not be observed by radars in Europe), we will use for the DRAO reference the median of the 3 daily observations at 17, 20 and 23 UTC, hence minimizing the probability of a flare contamination in the reference. By log-transforming both the radar observations (R) and the model reference values (M), then the selected score can simply be derived as the standard deviation of the differences in the logarithmic scale, $\sigma_{\mathrm{R-M}}$. Obviously, $\sigma_{\mathrm{R-M}}$ reaches the minimum, zero value, when R and M are perfectly correlated and the standard deviation of the radar observations, σ_{R}, is equal to the the standard deviation of the model estimates, σ_{M}. In formulas:

$$\sigma_{\mathrm{R-M}} = \sqrt{\sigma_{\mathrm{R}}^2 + \sigma_{\mathrm{M}}^2 - 2 \cdot r \cdot \sigma_{\mathrm{R}} \cdot \sigma_{\mathrm{M}}}, \tag{6}$$

where the expression inside the square root corresponds to the variance of the difference and r is the Pearson correlation coefficient between R and M expressed in dBsfu (i.e., log-transformed solar flux values).

The coefficient of determination, r^2, is another intuitive measure of agreement that can be interpreted as the proportion of the variation of the predictant that is "accounted for" or "explained" by the explanatory variable. We will express it in percentage

https://doi.org/10.5194/egusphere-2026-2097
Preprint. Discussion started: 21 May 2026
© Author(s) 2026. CC BY 4.0 License.

as follows:

$$\text{Explained variance}\,[\%] = 100\,r^2. \tag{7}$$

Finally, by normalizing $\sigma_{\mathrm{R-M}}$ using the dispersion of the model (M), it is possible to get a unitless score, which allows to compare intervals of strong solar activity with others close to the quiet Sun period. Such normalization is performed only as long as $\sigma_{\mathrm{M}} \leq \sigma_{\mathrm{R}}$, which is actually the case in all the cases analyzed in this manuscript. We will use for such dimensionless score the name Fractional Standard Deviation of the Error (FSDE), which corresponds to:

$$FSDE = \frac{\sigma_{\mathrm{R-M}}}{\sigma_{\mathrm{M}}}. \tag{8}$$

4.2 Monitoring and relative calibration of operational radar receivers

The aim of this subsection is to assess the performance of the two new models derived in Sect. 3.2 (scaling factor dependent on the solar activity) with respect to the (constant scaling factor) model operationally used in Europe, namely the model proposed by Tapping (2001) . We are using the same active period in 2014 analyzed in detail by Gabella et al. (2017): the focus is on two solar rotations showing comparable oscillations. Figure 4 shows, using black and grey lines, the solar flux density measured by three operational weather radars in Europe (two polarization states for the finnish Anjalankoski radar, ANJ, hence 4 lines overall). The standard deviation of radar observations, σ_{R}, is around 0.85 dB, with a minimum of 0.81 dB for Lema (vertical polarization) and a maximum of 0.88 dB for ANJ (horizontal polarization). As pointed out in Gabella et al. (2017), such dispersion is considerably larger than the one (0.63 dB) proposed by the operational model (red, dash-dot line) at 5.5 cm wavelength. The different amplitude (dispersion around the mean) between the red line and the 4 radar lines can be clearly seen. We note that, for the sake of simplicity, we are using here the (scaling factor and quiet Sun) values of Eq. (1) in Gabella et al. (2017) also for the finnish ANJ radar, whose wavelength is 5.3 cm, not 5.5 cm. If one used the slightly different, 5.3 cm values of Eq. (17) in Holleman et al. (2010b), the situation would be even worse: the standard deviation in this case results to be as small as 0.58 dB.

In the same figure, we also display (orange dash and blue solid lines) the estimated fluxes from the new models (scaling factor dependent on the solar activity). On the contrary, the amplitude of the oscillations of the two models, which visually look almost coincident (except for the maxima in the second rotation), look similar to those of the radars. In fact, it is 0.81 (0.78) dB for the blue (orange) line. Note that to derive the daily values of $p_\lambda(F_S)$ (see Eq. 3 and Eq. 5), we used the median of the three DRAO solar flux values available every day, not EOVSA (not yet available in 2014); hence, while the training in Sect. 3.2 was based on EOVSA data during solar cycle XXV, this evaluation is based on DRAO data during solar cycle XXIV. Adding up, we observe that all radars and models are able to observe the oscillation associated to the two solar rotations, which is intrinsically related to the fact that the entire solar microwave spectrum is predominantly modulated by the rotation of active regions. However, while Tapping (2001)'s model exhibits less variability, the new models show better agreement with the measurements, particularly in terms of amplitude of the oscillations. This is confirmed by the standard deviation of the differences between radars and models, whose values are reported in Tab. 1, together with the explained variance, listed between brackets in the same table.

https://doi.org/10.5194/egusphere-2026-2097
Preprint. Discussion started: 21 May 2026
© Author(s) 2026. CC BY 4.0 License.

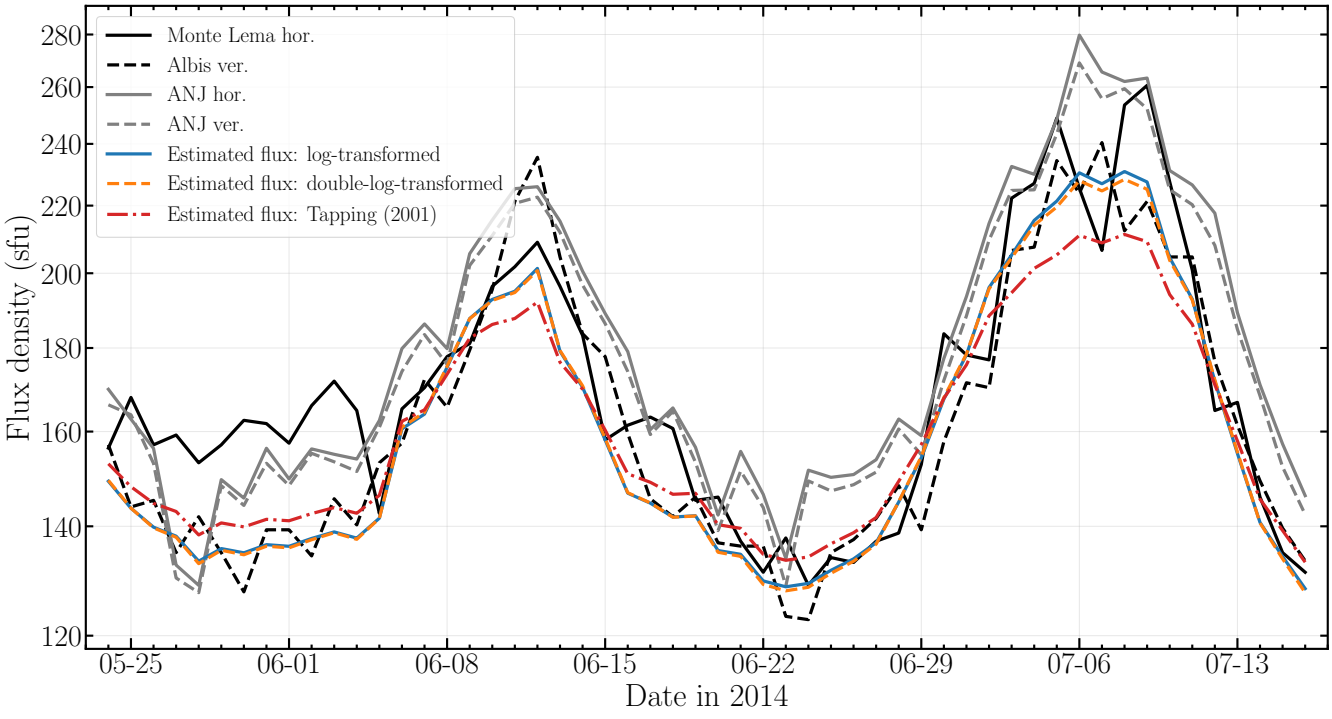

Figure 4. Solar flux density as a function of time over two solar rotations, clearly illustrating the slowly-varying component of the solar microwave emission (see Fig. 1). Actual measurements are derived from operational radars in the C-band: Monte Lema with horizontal polarization (solid black), Albis with vertical polarization, and Anjalankoski (ANJ) with both horizontal and vertical polarization (solid and dashed gray, respectively). The estimated flux densities from the models are also displayed: log-transformed model (solid blue), double-log-transformed model (dashed orange), and Tapping (2001) (dash-dotted red).

Table 1. Standard deviation of the differences and explained variance in percentage (in brackets) obtained by comparing operational radar measurements with the models in Fig. 4: 54 consecutive days (approximately two solar rotations) during the Sun active period in 2014

	Tapping (2001)[a]	**Log-transformed**[b]	**Double-log-transformed**[c]
Lema hor.	0.32 dB (84.7%)	0.32 dB (85.0%)	0.31 dB (84.8%)
Lema ver.	0.39 dB (78.3%)	0.38 dB (78.7%)	0.38 dB (78.5%)
Albis hor.	0.29 dB (90.2%)	0.26 dB (90.0%)	0.26 dB (90.2%)
Albis ver.	0.29 dB (91.0%)	0.25 dB (90.9%)	0.25 dB (91.0%)
ANJ hor.	0.31 dB (93.3%)	0.23 dB (93.3%)	0.23 dB (93.3%)
ANJ ver.	0.30 dB (93.2%)	0.23 dB (93.2%)	0.23 dB (93.2%)

[a] Estimates using the constant p_λ from Tapping (2001).

[b] Estimates using the varying p_λ with the log-transformed model in Eq. (3).

[c] Estimates using the varying p_λ with the double-log-transformed model in Eq. (5).

https://doi.org/10.5194/egusphere-2026-2097
Preprint. Discussion started: 21 May 2026
© Author(s) 2026. CC BY 4.0 License.

Table 2. FSDE in Eq. (8) obtained by comparing operational radar measurements with the models in Fig. 4: 54 consecutive days (approximately two solar rotations) during the Sun active period in 2014.

	Tapping (2001)[a]	Log-transformed[b]	Double-log-transformed[c]
Lema hor.	0.51	0.39	0.41
Lema ver.	0.62	0.47	0.49
Albis hor.	0.46	0.32	0.33
Albis ver.	0.46	0.31	0.32
ANJ hor.	0.49	0.28	0.29
ANJ ver.	0.48	0.28	0.29

[a] Estimates using the constant p_λ from Tapping (2001).

[b] Estimates using the varying p_λ with the log-transformed model in Eq. (3).

[c] Estimates using the varying p_λ with the double-log-transformed model in Eq. (5).

Table 1 shows that all radars exhibit smaller standard deviations of the differences when using the log-transformed models instead of the model by Tapping (2001), indicating that the models with varying $p_\lambda(F_S)$ agree considerably better with the solar flux densities observed by the radars, particularly Albis and ANJ. By noting the lower correlation between Lema radar and the models, one would expect a larger standard deviation of the differences for this radar, which is, in fact, the case. A careful observer of Fig. 4 would point out that from May 24 to June 4 (twelve days), the Lema (horizontal polarization) signal overestimates the flux, while it is much closer to the models later on, due to an apparent drop of approximately -0.7 dB on June 5. Unfortunately, we cannot confirm nor deny that the gain of the Low-Noise Amplifiers was approximately 0.7 dB larger than the proper value; however, we can say that after having reduced (during such twelve days) Lema solar flux values by 0.7 dB, then the coefficient of determination of (for instance) the log-transformed model increases from 0.847 to 0.926, while the standard deviation of the differences decreases from 0.32 dB to 0.24 dB, which represents indeed a remarkable improvement.

Table 2 shows the normalized standard deviation of the differences, which is the FSDE as defined in Eq. (8): also in this case, the best (worst) performance is obtained by the ANJ (Lema) radar. The values of the Albis radar are of particular interest for a comparison between the performance obtained with Sun-Check and 54 consecutive days in this section and the Sun-Track results (20 days in 13 years) in the next Section. For instance (horizontal polarization), we will see in Sect. 4.3 that the performance will improve from a FSDE triplet equal to (0.46, 0.32, 0.33) to a better triplet (0.21, 0.14, 0.14).

4.3 Absolute calibration of dual-polarization radar receiver chains

We now use the models within the framework of the absolute calibration of dual-polarization weather radar receivers. As stated, we rely on much thinner datasets based on accurate Sun-Track measurements. Among the 5 MeteoSwiss radars, the one with the largest dataset is Albis; all the 20 on-demand, Sun-Track measurements performed using the Albs receiver chains, (from November 2013 until March 2025, comprising solar cycles XXIV and XXV) have been performed with the same Calibration Unit. This means same internal reference Noise Source and same Low-Noise Aplifiers.

https://doi.org/10.5194/egusphere-2026-2097
Preprint. Discussion started: 21 May 2026
© Author(s) 2026. CC BY 4.0 License.

Figure 5 shows the comparison between the accurate Sun-Track values of the measured solar flux densities from Albis and the corresponding C-band fluxes estimated from the various models, which transform the median of the 3 daily DRAO measurements into C-band references. For both polarizations, the models exhibit an excellent linear relationship with the radar measurements, confirming that the variability of the solar flux mainly due to the slowly varying component is well captured by all models. The slopes of the linear fits are close to unity, particularly for the log-transformed models, indicating that these models better reproduce the dynamical range of the radar measurements, corroborating the results derived in the previous section. The explained variance of the six linear regressions is shown between brackets in Tab. 3, together with the most important score within the framework of absolute calibration: the geometric Bias, which is the average of the differences expressed in dB. It is a geometric average because the usual (arithmetic) average has been applied to values on the log-transformed, dBsfu, scale. Alternatively, one could first derive the average values in sfu of both the radar and the models, then log-transform their ratio, hence obtaining the mean Bias in dB. In this specific case, since the standard deviation of the five signals (two polarization states for the radar and three models) is bounded between 0.7 and 0.8 dB, the geometric Bias and mean Bias are coincident in the four cases where the log and the double-log model are used as reference. However, when the Tapping (2001)'s model is used as a reference, they just differ by 0.02 and 0.01 dB. The geometric Bias of the radar measurements ranges between -1.15 to -0.76 dB depending on polarization and model. Consistent with the trends observed in Fig. 5, the log-transformed models systematically yield smaller absolute discrepancies than Tapping (2001)'s model, with smaller underestimation of the order of 0.05–0.06 dB. This reduction reflects the better alignment of the log-transformed models with the absolute amplitude of the radar measurements.

Table 3. Albis absolute calibration results: quantitative assessment of the geometric Bias using DRAO S-band solar flux values as reference, extrapolated to C-band with three different models. The explained variance in percentage is also shown between brackets

	Tapping (2001)	**Log-transformed**	**Double-log-transformed**	**# of Sun tracks**
Albis hor.	-1.15 dB (97.8%)	-1.09 dB (98.3%)	-1.10 dB (98.3%)	20
Albis ver.	-0.82 dB (96.6%)	-0.76 dB (96.9%)	-0.77 dB (96.9%)	20

There are two important conclusions coming out of this absolute calibration exercise:

- both polarization channels of Albis radar underestimate the solar flux when using DRAO S-band values extrapolated to C-band as reference; the underestimation seems to be a bit more (less) than 1 dB for the horizontal (vertical) polarization;
- there is an undesired, residual Bias between the polarization states of the order of 0.3 dB.

From a quantitative, polarimetric point of view, a possible miscalibration of 0.3 dB affecting the differential reflectivity is worse than a possible underestimation of 1 dB affecting the radar reflectivity, Z. Furthermore, the miscalibration between H and V has also been confirmed by extensive analysis during light rain events. Consequently, an offset of +0.3 dB has been promptly inserted in the Zdr product of Albis radar more than 10 years ago. In the future, MeteoSwiss may consider to re-adjust the

https://doi.org/10.5194/egusphere-2026-2097
Preprint. Discussion started: 21 May 2026
© Author(s) 2026. CC BY 4.0 License.

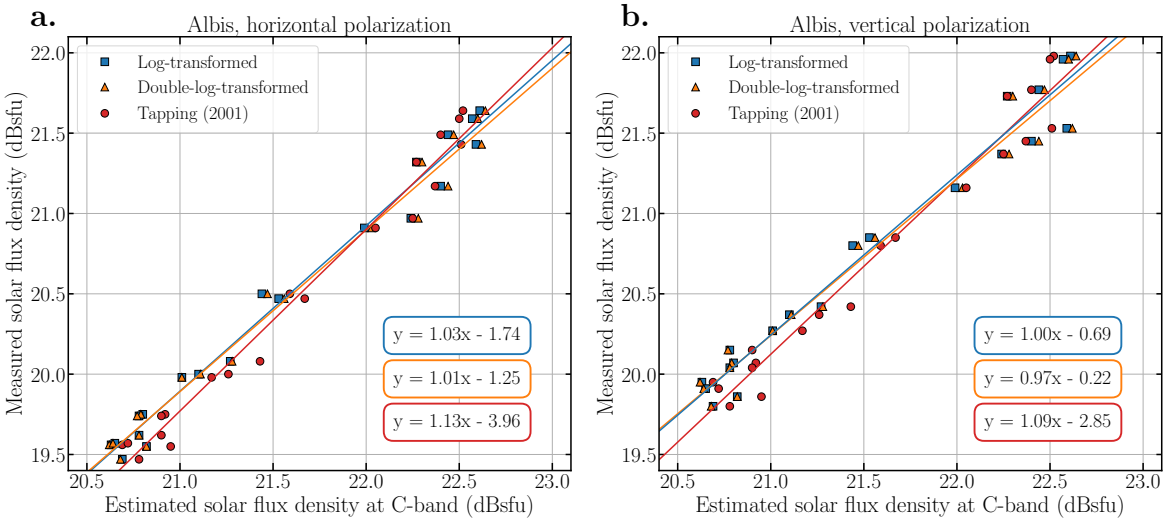

Figure 5. Comparison of the absolute calibration of measured solar flux densities from Albis (horizontal polarization in panel (*a*) and vertical polarization in panel (*b*)) with the estimated flux densities derived from DRAO measurements scaled to C-band using different models (see legend). The scatter points represent individual data points, while the solid lines show linear fits to the data. Note that there is a systematic offset of approximately 1 dBsfu between the measured and estimated values due to instrumental effects (see Sect. 4.3).

calibration constant of both receiver channels, hence bringing the Bias of both polarizations closer to zero and removing the current 0.3 dB offset in Zdr.

Table 4 shows the standard deviation of the differences in dB and the corresponding dimensionless FSDE values (in brackets) for the 6 cases: the new models perform better, yielding values as small as ±0.11 dB ($FSDE = 0.14$) for the horizontal polarization. This confirms that the model captures the short-term and day-to-day variations in the measured solar flux densities.

Table 4. Albis absolute calibration results: uncertainties of the Bias expressed in terms of standard deviation of the differences in dB and of the unitless FSDE (in brackets), see Eq. (8).

	Tapping (2001)	**Log-transformed**	**Double-log-transformed**
Albis hor.	±0.15 dB (0.21)	±0.11 dB (0.14)	±0.11 dB (0.14)
Albis ver.	±0.16 dB (0.23)	±0.14 dB (0.18)	±0.14 dB (0.18)

5 Discussion

This section is organized in three parts. We start with a short example regarding how additional accurate Sun-Track measurements can be set up in the context of the absolute calibration of a weather radar; for the sake of brevity, the example deals with

https://doi.org/10.5194/egusphere-2026-2097
Preprint. Discussion started: 21 May 2026
© Author(s) 2026. CC BY 4.0 License.

the Albis horizontal polarization. Then, the most important subsection: a preliminary analysis of the performance of absolute calibration using reference flux values acquired at the same time of the radar Sun-Track and, most of all, almost at the same frequency. Finally, we are presenting a possible physical interpretation of the new model(s) having a scaling factor that depends on the solar activity.

5.1 Prediction of the solar flux values that Albis could have measured on a given day this year, e.g., March 5, 2026

Given the previously 20 Sun-Track measurements acquired in the years between 2013 and 2025 and knowing the DRAO reference value at S-band in a day of the current year (e.g., March 5, 2006), can we somehow predict the Sun-Track value that Albis radar has recorded at C-band for this specific day? The answer to this simple question is affirmative. For instance, Knowing that on March 7, 2025, which is the day of the last Sun-Track value analyzed in Sect. 4.3, the median value delivered by DRAO at S-band was 147.3 sfu, which is almost the same as on March 5, 2026 (146.2 sfu) and assuming a stable radar receiver (1-year, "long-term" persistence), one could expect on March 5 a value at C-band close to what has been measured on March 7, 2025, which was 21.17 dBsfu (horizontal polarization). To complete the exercise, one could use the knowledge of the models derived in this work: for instance, using Eq. (1) (146.2 sfu corresponds to 22.35 dBsfu at C-band) and Eq. (3) (146.2 sfu corresponds to 22.38 dBsfu at C-band) and the corresponding linear fit in Fig 5(a) (horizontal polarization), one gets a prediction of 21.30 and 21.31 dBsfu, respectively (21.38 with the double-log-transformed model). The actual value measured by the radar was 21.18 dBsfu, which is, for instance, within the uncertainty level associated to the prediction of the Tapping (2001) model (± 0.15 dB).

5.2 Absolute calibration of Albis radar using solar flux values measured directly at 5 GHz

The RSTN comprises four sites having very different longitude (Hawaii, MA, Italy, Australia) supplying, among other, daily noon flux measurements at 8 discrete frequencies. One of them is located at 4995 MHz (6 cm), which is very close to the frequency of our weather radars. As stated, for best radar calibration, it is recommended to use measurements acquired at the same time and, most of all, almost at the same frequency. In this respect, in our case, the best site is certainly San Vito (SVTO) dei Normanni (southeastern part of Italy). Out of the 20 Sun-Track days used in Sect. 4.3, daily noon flux measurements are available in 19 cases. In order to have the same number of samples as in Sect. 4.3, we have thought of replacing the missing date with the additional Sun-Track recently acquired (March 5, 2026) and described in Sect. 5.1. A first peculiarity of SVTO reference flux values is represented by the relatively large dispersion tof such referemce: the standard deviation of the 20 SVTO values is 1.1 dB, which is 0.3 larger than the standard deviation of the corresponding radar estimates. Consequently, the comparison with the performance obtained in Sect. 4.3 can be done in terms of uncertainties in dB, but not in terms of unitless FSDE. Using SVTO as a reference, one gets the results listed in Tab. 5. Somehow surprisingly, uncertainties (central column) are larger than what obtained in Sect. 4.3, where DRAO is the reference (see Tab. 4). Also the explained variance is worse. Similarly to what obtained in Sect. 4.3, the Bias values (first column) show that the underestimation affects both polarization states, horizontal more than vertical. Although a bit more underestimated, the horizontal channel is affected by a

https://doi.org/10.5194/egusphere-2026-2097
Preprint. Discussion started: 21 May 2026
© Author(s) 2026. CC BY 4.0 License.

smaller uncertainty and is better correlated with the reference also according the SVTO 6-cm reference. However, according to SVTO, the underestimation that affects both channels is worse by approximately 0.3 dB, with a larger associated uncertainty.

Table 5. Absolute calibration results for Albis using C-band RSTN noon fluxes acquired in San Vito dei Normanni.

	Bias (Expl. Var.)	**Uncertainty**	**# of Sun tracks**
Albis hor.	-1.41 dB (85.4%)	±0.46 dB	20
Albis ver.	-1.08 dB (80.8%)	±0.51 dB	20

Why does a larger uncertainty affect SVTO results, despite the acquisition directly at C-band? On the one hand, we do not have details regarding the integration time of the RSTN noon flux values nor regarding the adopted strategy to subtract the noise. On the other hand, the integration time of DRAO is as long as 1 hour. Furthermore, DRAO has implemented an original scan strategy, which minimizes, through subtraction, increased Noise influences of the environment through the secondary lobes. Such method is illustrated in Fig. 6 at page 398 of Tapping (2013). We think that these differences (improved Sun-to-Noise ratio thanks to longer integration time; optimized scan strategy for Noise cancellation) could explain the, somehow unexpected, lower performance obtained with SVTO as a reference with respect to the comparison with our models in Sect. 4.3. This highlights the importance not only of using solar flux values measured directly at C-band at about the same time, but also that of adopting an optimized radio telescope scan strategy.

5.3 On the origin of the varying frequency of the peak of the slowly-varying component

In order to understand the behavior of the slowly-varying component, we need to discuss the evolution of its spectral shape with solar activity. This is closely related to the validity of the second assumption in Tapping (2001)'s model, which states that as solar activity rises and falls, the amplitude of the spectrum changes while its shape remains nearly unchanged. Our results, combined with the EOVSA spectra shown in Fig. 2, demonstrate that this assumption is only partially satisfied, and that deviations in the spectral shape have a direct impact on the value of p_λ. These considerations motivated the implementation of a varying p_λ as a function of the solar flux (see Sect. 3.2).

As illustrated in Fig. 2, the spectrum of the slowly-varying component does not only vary in amplitude but also exhibits clear changes in spectral shape. An explanation lies in the intrinsic physical properties of the active regions that dominate the emission. The slowly-varying component at microwave frequencies is produced primarily by gyromagnetic emission, whose frequencies depend on the local magnetic field strengths within active regions. This can be seen from the expression of the electron gyrofrequency f_e (c.f., Benz, 2002),

$$f_\mathrm{e} = \frac{q}{2\pi m_\mathrm{e} c} B \simeq 2.8\, B \text{ MHz}, \tag{9}$$

where q is the electron charge, m_e is the electron mass, B the magnetic flux density, and c the speed of light. Please note that the magnetic flux density in the equation above is not expressed in Tesla (Int. Sys. of Units) rather in Gauss (Gaussian-cgs Unit). The expression follows directly from the Lorentz force acting on a charged particle in a homogeneous magnetic field

https://doi.org/10.5194/egusphere-2026-2097
Preprint. Discussion started: 21 May 2026
© Author(s) 2026. CC BY 4.0 License.

(Benz, 2002). The gyrofrequency sets the fundamental scale for solar microwave emission and shows that stronger magnetic fields shift the characteristic emission to higher frequencies.

A further refinement concerns the role of gyroresonance harmonics. Gyromagnetic radiation at microwave wavelengths is emitted at harmonics of the gyrofrequency, $f \approx s f_e$, where $s = 2, 3, 4, \ldots$ (Melrose, 1980). For typical solar active regions, the lowest harmonics ($s \leq 3$) dominate the opacity and therefore shape the observable spectral peak of the slowly-varying component (White and Kundu, 1997). At higher harmonics, the emitting layer becomes more transparent (optically thin), so those harmonics add less to the peak brightness (Gary and Hurford, 2004). Consequently, the observed peak frequency is mainly shaped by the harmonics that remain optically thick for the magnetic field distribution present in the active region.

A simple example illustrates the physical origin of this spectral evolution. If on the solar disk there is a single, isolated active region with magnetic fields clustered around $B \approx 1\,\mathrm{kG}$, the peak of the slowly-varying component would lie around $2.8\,\mathrm{GHz}$, which happens to be the exact observing frequency of the DRAO solar flux monitor. In more realistic situations, however, the solar disk, especially around the maximum activity of the 11-year solar cycle, contains multiple and far more complex active regions with a broad range of magnetic field strengths. If the dominant emission arises from fields around $B \approx 1.5\,\mathrm{kG}$, the spectral peak shifts upward to about $4.5\,\mathrm{GHz}$, therefore at frequencies between the S- and C-band. Such shifts in the peak frequency directly influence the scaling for estimating the flux at C-band with the DRAO S-band measurements, and therefore modify p_λ. The models proposed in this study capture part of this behavior by allowing p_λ to vary as a function of the observed flux level, thereby extending Tapping (2001)'s model to account for physically motivated changes in the spectral shape of the slowly-varying component.

6 Summary, conclusions and outlook

The results presented in this study corroborate that the Tapping (2001) model, widely used in Europe for the monitoring and calibration of operational weather radars using the DRAO 10.7 cm solar flux measurements, remains a robust and reliable approach, as already shown in previous studies (e.g., Holleman et al., 2010b, a; Gabella et al., 2014; Huuskonen et al., 2016; Gabella et al., 2017). The model successfully estimates the C-band solar flux reference values with differences smaller than 1 dB, as originally intended. The central aim of this work was to investigate whether the method can be further improved by revisiting one of its underlying assumptions, namely, that as solar activity varies, the amplitude of the solar microwave spectrum changes, while its spectral shape remains nearly invariant. Our analysis, based on wide-band solar observations by EOVSA, shows that this assumption holds only partially. Thanks to EOVSA observations of the slowly-varying component, we show that the spectral shape does indeed evolve with the solar activity, driven primarily by changes in the magnetic field distributions of the active regions responsible for the emission. This motivates a refinement of the original model of Tapping (2001); the novel models retain the physical foundation but permits its scaling parameter p_λ to vary with the solar flux level. This is indeed the key distinction between the model of Tapping (2001), where p_λ is fixed, and the models proposed in this article. This extension is physically motivated by the changing peak frequency of the slowly-varying component and is designed to preserve the conceptual simplicity and operational applicability of the original method while accounting, to some extent,

https://doi.org/10.5194/egusphere-2026-2097
Preprint. Discussion started: 21 May 2026
© Author(s) 2026. CC BY 4.0 License.

for spectral changes. In particular, we have modeled an exponential and a double-exponential dependence between p_λ and the solar activity.

The results obtained in this article led us to the following conclusions:

- The proposed models with varying p_λ capture a larger dynamical range between the local minima and maxima of the solar flux density, with differences of the order of 5–10% (linear) compared to the model with fixed p_λ of Tapping (2001).
- The performance of the relative calibration shows for Albis (ANJ) radar a decrease of the Fractional Standard Deviation of the error from approximately 0.5 to (less than) 0.3; for the horizontal (vertical) polarization of the Lema radar, the FSDE improves from 0.5 (0.6) to less than 0.4 (0.5).
- In the case of absolute calibration of the Albis radar, the FSDE improves from 0.21 (0.23) to 0.14 (0.18) for the horizontal (vertical) polarization.

The results have shown that, on the one hand, the original model by Tapping (2001) is already robust; on the other hand, the refinements introduced in this work move in the right direction by incorporating physically motivated spectral variability. Whether these improvements are significant ultimately depends on the specific application. With the rapid development of artificial intelligence and the need for prompt, fully-automatic end-to-end applications, the demands on the stability and calibration of the radar hardware are increasing considerably. The best result obtained so far thanks to the Sun-Track technique (FSDE as small as 0.14) could represent a remarkable benchmark: we think that such degree of agreement could not be easily further improved, unless measuring the slowly varying component at the same time and, most of all, in the same frequency band used by the radars. As pointed out in Sec. 8 and 9.3 of Tapping (2013), the best approach consists certainly in complementing the above mentioned analysis by directly measuring the solar flux in the same frequency band used by the radars. In Europe, solar measurements acquired at 4995 MHz (hence only 500 MHz aside) are available thanks to the SVTO-RSTN radio telescope, located in San Vito dei Normanni in Italy: the agreement between Albis and SVTO (Sun-Track technique, absolute calibration) in terms of FSDE is of the order of 0.42 dB (Horizontal polarization). Our final recommendation is that of developing and installing an optimized C-band radio telescope in Europe tailored to radar calibration purposes and operating at 5.4 GHz (and/or 5.6 GHz) to complement SVTO observations at 5 GHz.

Data availability. EOVSA and DRAO observations are publicly available (see Sect. 2.1). Operational weather radar data can be provided upon request.

Video supplement. A video supplement of Fig. 1 is publicly available with the following DOI: https://doi.org/10.5446/73084.

https://doi.org/10.5194/egusphere-2026-2097
Preprint. Discussion started: 21 May 2026
© Author(s) 2026. CC BY 4.0 License.

Author contributions. The EOVSA data analysis and the derivation of the varying p_λ parameter has been performed by AFB. MG derived the two log-transformed models and performed the comparison with the operational radars. Both authors contributed to the interpretation of the results and the writing of the manuscript.

Competing interests. The authors declare that no competing interests are present.

Acknowledgements. Thanks are due to several scientists in the last decade for useful and stimulating discussions regarding the use of the Sun as a calibration source not only for monitoring, but even for the absolute calibration of dual-polarization weather radar receivers: Asko Huuskonen, Iwan Holleman, Mikko Kurri, Annakaisa Von Lerber, Michael Frech, Jose Nicolas Gonzalez Perez, Axel Murk, Philipp Schmid, Maurizio Sartori, Marco Boscacci, Daniel Wolfensberger, Simone Balmelli, Urs Germann. MG would like to warmly thank the NRC of Canada and in particular Ken Tapping and Andrew Grey for the fruitful, instructive and unforgettable experience during the visit at the DRAO / Herzberg Astronomy and Astrophysics National Research Council Canada, together with Urs, Axel and Philipp, in August 2024 (a quite active Sun period!). In addition, the authors would like to thank Dale Gary for helpful discussions regarding EOVSA observations and Simone Balmelli for commenting on the final draft of the paper. IRSOL is supported by the Swiss Confederation (SERI), Canton Ticino, the city of Locarno and the local municipalities. The Expanded Owens Valley Solar Array (EOVSA) was designed and built and is now operated by the New Jersey Institute of Technology (NJIT) as a community facility. AFB is supported by the Swiss National Science Foundation (SNSF) grant 200020_213147.

https://doi.org/10.5194/egusphere-2026-2097
Preprint. Discussion started: 21 May 2026
© Author(s) 2026. CC BY 4.0 License.

References

Benz, A. O.: Plasma astrophysics: Kinetic processes in solar and stellar coronae, Springer, 2002.

Benz, A. O.: Radio Emission of the Quiet Sun, Landolt Börnstein, 4B, 103, https://doi.org/10.1007/978-3-540-88055-4_5, 2009.

Frush, C. L.: Using the sun as a calibration aid in multiple parameter meteorological radars, in: IN: Conference on Radar Meteorology, pp. 306–311, 1984.

Gabella, M.: Checking absolute calibration of vertical and horizontal polarization weather radar receivers using the solar flux, J. Electr. Eng, 3, 163–169, 2015.

Gabella, M. and Leuenberger, A.: Dual-polarization observations of slowly varying solar emissions from a mobile X-Band radar, Sensors, 17, 1185, 2017.

Gabella, M., Sartori, M., Boscacci, M., and Germann, U.: Vertical and horizontal polarization observations of slowly varying solar emissions from operational Swiss weather radars, Atmosphere, 6, 50–59, 2014.

Gabella, M., Huuskonen, A., Sartori, M., Holleman, I., Boscacci, M., and Germann, U.: Evaluating the Solar Slowly Varying Component at C-Band Using Dual-and Single-Polarization Weather Radars in Europe, Advances in Meteorology, 2017, 4971 765, 2017.

Gary, D. E. and Hurford, G. J.: Radio Spectral Diagnostics, in: Astrophysics and Space Science Library, edited by Gary, D. E. and Keller, C. U., vol. 314 of *Astrophysics and Space Science Library*, p. 71, https://doi.org/10.1007/1-4020-2814-8_4, 2004.

Gary, D. E., Chen, B., Dennis, B. R., Fleishman, G. D., Hurford, G. J., Krucker, S., McTiernan, J. M., Nita, G. M., Shih, A. Y., White, S. M., and Yu, S.: Microwave and Hard X-Ray Observations of the 2017 September 10 Solar Limb Flare, , 863, 83, https://doi.org/10.3847/1538-4357/aad0ef, 2018.

Giersch, O. and Kennewell, J.: Analysis of the Radio Solar Telescope Network's Noon Flux Observations Over Three Solar Cycles (1988-2020), Radio Science, 57, e2022RS007456, https://doi.org/10.1029/2022RS007456, 2022.

Guidice, D. A., Cliver, E. W., Barron, W. R., and Kahler, S.: The Air Force RSTN System, in: Bulletin of the American Astronomical Society, vol. 13, p. 553, 1981.

Holleman, I. and Beekhuis, H.: Weather radar monitoring using the sun, KNMI, 2004.

Holleman, I., Huuskonen, A., Gill, R., and Tabary, P.: Operational monitoring of radar differential reflectivity using the sun, journal of Atmospheric and Oceanic Technology, 27, 881–887, 2010a.

Holleman, I., Huuskonen, A., Kurri, M., and Beekhuis, H.: Operational monitoring of weather radar receiving chain using the sun, Journal of Atmospheric and Oceanic Technology, 27, 159–166, 2010b.

Huuskonen, A. and Holleman, I.: Determining weather radar antenna pointing using signals detected from the sun at low antenna elevations, Journal of Atmospheric and Oceanic Technology, 24, 476–483, 2007.

Huuskonen, A., Kurri, M., and Holleman, I.: Improved analysis of solar signals for differential reflectivity monitoring, Atmospheric Measurement Techniques, 9, 3183–3192, 2016.

Kennewell, J. A.: Solar radio interference to satellite downlinks, in: International Conference on Antennas and Propagation (ICAP 89), pp. 334–339, 1989.

Melrose, D. B.: Plasma astrophysics, vol. 1, CRC Press, 1980.

Pratte, J. F. and Ferraro, D. G.: Automated solar gain calibration, in: IN: Conference on Radar Meteorology, pp. 619–622, 1989.

Schmid, P. J., Sartori, M., Gabella, M., Renker, M., Wolfensberger, D., Kotiranta, M., and Murk, A.: Scattering parameters of a wet radome, International Journal of Microwave and Wireless Technologies, 17, 862–873, 2025.

https://doi.org/10.5194/egusphere-2026-2097
Preprint. Discussion started: 21 May 2026
© Author(s) 2026. CC BY 4.0 License.

Shaik, S. B. and Gary, D. E.: Implications of Flat Optically Thick Microwave Spectra in Solar Flares for Source Size and Morphology, , 919, 44, https://doi.org/10.3847/1538-4357/ac0fdb, 2021.

Tapping, K.: Antenna Calibration Using the 10.7 cm Solar Flux, in: Workshop on Radar Calibration, Albuquerque NM, American Meteor Society, 2001.

Tapping, K. F.: The 10.7 cm solar radio flux (F10.7), Space Weather, 11, 394–406, https://doi.org/https://doi.org/10.1002/swe.20064, 2013.

White, S. M. and Kundu, M. R.: Radio Observations of Gyroresonance Emission from Coronal Magnetic Fields, , 174, 31–52, https://doi.org/10.1023/A:1004975528106, 1997.

Wilks, D. S.: Statistical methods in the atmospheric sciences, vol. 100, Academic press, 2011.

Yun, Y., Park, Y.-S., Kim, C.-H., Lee, B., Kim, J.-H., Yoo, S., Lee, C.-H., Han, J., and Kim, Y. Y.: Development of 2.8-GHz solar flux receivers, , 47, 201–207, 2014.